High energy heavy ion jets emerging from laser plasma generated by long pulse laser beams from the NHELIX laser system at GSI

G. SCHAUMANN,[1] M.S. SCHOLLMEIER,[1] G. RODRIGUEZ-PRIETO,[2] A. BLAZEVIC,[2]
E. BRAMBRINK,[1,6] M. GEISSEL,[1,7] S. KOROSTIY,[2] P. PIRZADEH,[1] M. ROTH,[1] F.B. ROSMEJ,[3]
A.YA. FAENOV,[4] T.A. PIKUZ,[4] K. TSIGUTKIN,[5] Y. MARON,[5] N.A. TAHIR,[2]
AND D.H.H. HOFFMANN[1,2]

[1]Technische Universität Darmstadt, Darmstadt, Germany
[2]GSI, Darmstadt, Germany
[3]Université de Provence et CNRS, Marseille, France
[4]Multicharged Ions Spectra Data Center, VNIIFTRI, Moscow, Russia
[5]Weizmann Institute of Science, Rehovot, Israel
[6]Current address: Ecole Polytechnique, Paris.
[7]Current address: Sandia National Laboratories, Albuquerque, New Mexico.

Abstract

High energy heavy ions were generated in laser produced plasma at moderate laser energy, with a large focal spot size of 0.5 mm diameter. The laser beam was provided by the 10 GW GSI-NHELIX laser systems, and the ions were observed spectroscopically in status nascendi with high spatial and spectral resolution. Due to the focal geometry, plasma jet was formed, containing high energy heavy ions. The velocity distribution was measured via an observation of Doppler shifted characteristic transition lines. The observed energy of up to 3 MeV of F-ions deviates by an order of magnitude from the well-known Gitomer (Gitomer *et al.*, 1986) scaling, and agrees with the higher energies of relativistic self focusing.

Keywords: Dense plasma; Laser-plasma ion source; spectroscopy

1. INTRODUCTION

The generation of high energy ion beams (Zhidkov *et al.*, 1999; Pegoraro *et al.*, 2004; Shorokhov & Pukhov, 2004; Balakirev *et al.*, 2004; Malka & Fritzler, 2004), and high energetic and intense X-ray bursts (Magunov *et al.*, 2003; Fukuda *et al.*, 2004) is a well known phenomenon in interaction processes of short and ultra-short laser pulses with matter. Ion generation from laser plasmas with long laser pulses and comparatively low power was studied by many groups recently (Stepanov *et al.*, 2002; Rafique *et al.*, 2006; Khaydarov *et al.*, 2005). This is partly due to the fact that these ions have a great potential as powerful ion sources for heavy ion accelerators (Haseroth & Hora, 1996; Alexeev *et al.*, 2002; Ogawa *et al.*, 2003). While in both cases the underlying phenomenon of particle production seems to be quite different, it is a non equilibrium process in both cases which gives rise to the fast ion emission process.

The interest in laser plasmas and interaction phenomena of heavy ion beams with ionized matter at the GSI heavy ion accelerator laboratory stems from the fact that heavy ion beams are viewed as a potential driver for inertial fusion (Sharkov, 2002; Koshkarev, 2002; Hoffmann *et al.*, 2000). Thus there is a tradition to investigate accelerator related issues like beam transport phenomena in laser plasma channels (Penache *et al.*, 2002), and interaction processes of heavy ion beams with dense, beam heated matter (Varentsov *et al.*, 2003). From earlier experiments with fully ionized hydrogen discharge and pinch plasmas it is well known, that ionized matter has an increased stopping power for heavy ions (Hoffmann *et al.*, 1990; Jacoby *et al.*, 1995; Roth *et al.*, 2000; Hasegawa *et al.*, 2003), and that the charge state of heavy ion beams passing through plasma is considerably altered (Dietrich *et al.*, 1992). In order to achieve plasma parameters which extend far beyond those of discharge and

pinch plasmas a laser Nd: glass laser system with total laser beam pulse energy well above 100 J was installed. The need for high laser energy in ion-beam laser-plasma experiments is quite obvious, since the diameter of the ion beam is on the order of 1 mm, and therefore the laser plasma has at least to be as large, or even larger to avoid steep temperature and density gradients in the interaction zone. Currently at GSI laser systems with a kilojoule beam and petawatt capability (Neumayer *et al.*, 2004) is under construction for high energy density physics experiments with intense laser and particle beams (Hoffmann *et al.*, 2005).

2. THE NHELIX LASER SYSTEM AT GSI

The first high energy laser system that became operational at GSI is the nanosecond high energy laser for heavy ion experiments (NHELIX). This system has recently been improved significantly. Due to major changes in the system layout, the quality in terms of temporal and spatial beam homogeneity was improved, while at the same time the output energy was raised to 120 J. This could be achieved with the available number of amplifiers, which significantly brought down the cost for the upgrade. Moreover, a second front-end with shorter pulse length was integrated into the laser amplifier chain. Therefore the NHELIX system is now capable of delivering one beam with 120 J in 14 ns (ns-beam), while the second beam line is still under construction and is supposed to provide 5 J in 0.5 ns (sub ns-beam).

The power level of these two beams is of the same order of magnitude; their application at the plasma physics experiments is different. The high energy pulse with rather long pulse duration is primarily used to generate a high density plasma from thin solid state targets, while the second beam with short pulse length in comparison to the heating pulse and the timescale on which the hydrodynamic expansion of the plasma takes place, serves as a diagnostic tool. This more complex and versatile setup enables a great variety of experiments in the field of plasma physics, especially in combination with the petawatt high energy laser for heavy ion experiments (PHELIX) laser, which is expected to deliver first light on the kJ level to the experimental area by the end of 2005 (Neumayer *et al.*, 2005).

The actual laser configuration is of the master oscillator-pulsed amplifier (MOPA) type. A master oscillator (Nd:YAG) generates a low energy pulse for amplification, that is followed by rod amplifiers (silicate-glass), whose diameter increase stepwise up to 64 mm for the last amplifier. As the laser light fluence is well below the saturation level, the same amplifier can be used multiple times to increase the energy of a beam, e.g., in a double pass configuration, or one can even use the same amplifier to gain energy for pulses coming from different oscillators. The latter configuration was realized with the first two amplifiers; see Figure 1 for the outline of the NHELIX laser system and Table 1 for an overview of the main optical components.

Laser beams, ns-beam as well as the sub-ns beam are launched into the first amplification section. The insertion is done with a thin film polarizer that transmits the ns-beam (p-polarized) and reflects the sub-ns beam which is impinging under the Brewster-angle with s-polarization. Since
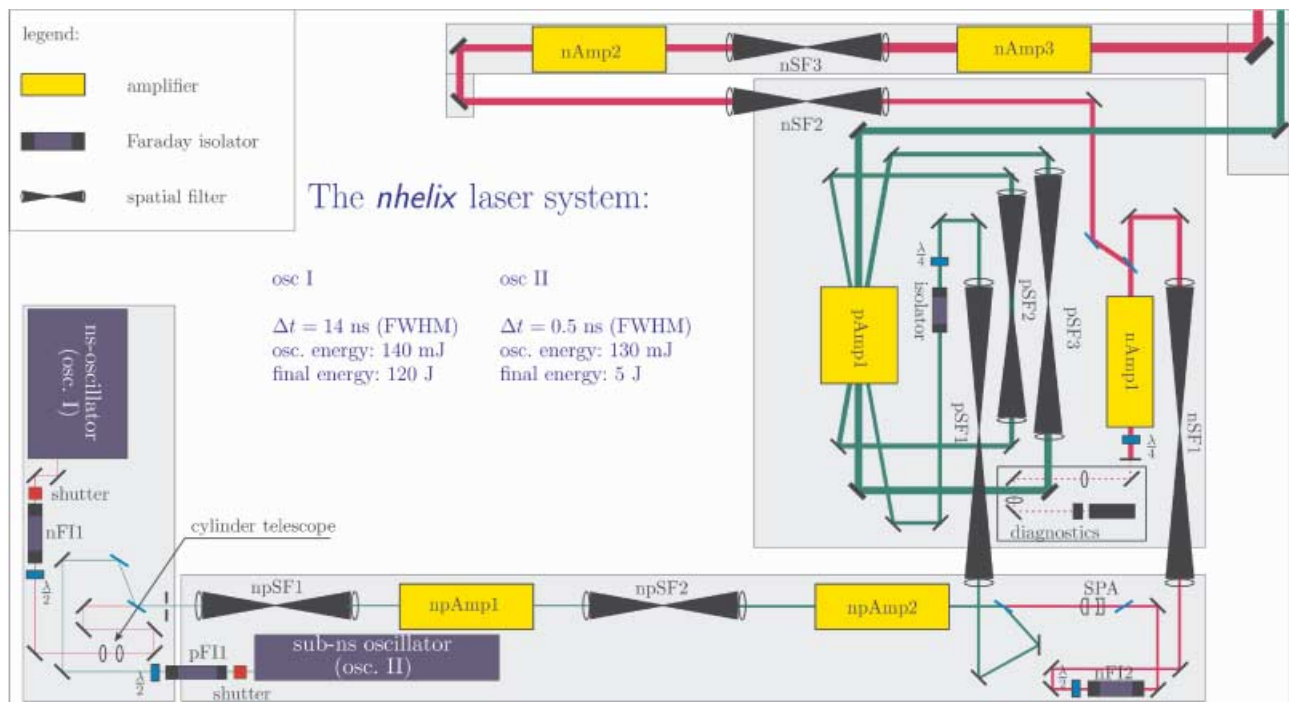

Fig. 1. Outline of the NHELIX laser system.

Table 1. *Main optical components of the NHELIX laser system (Please see Fig. 1 for abbreviations.)*

	Long pulse chain				Short pulse chain		
	d [mm]	magn.	L [mm]		d [mm]	magn.	L [mm]
isolator: nFI1	10.00			isolator: pFI1	10.00		
npSF1		1.60	656	npSF1		1.60	656
npAmp1	15.87		220	npAmp1	15.87		220
npSF2		1.61	658	npSF2		1.61	658
npAmp2	25.40		232	npAmp2	25.40		232
SPA	24.00						
isolator: nFI2	25.00						
nSF1		1.19	1525	pSF1		1.11	1922
nAmp1	32.00		475	pAmp1	44.50		235
nAmp1	32.00			pSF2		1.12	1719
nSF2		1.54	684	pAmp1	44.50		235
nAmp2	45.00		450	pSF3		1.33	1770
nSF3		1.43	855	pAmp1	44.50		235
nAmp3	64.00		680	pSF4		1.00	4056

these beams are propagating parallel but with perpendicular polarization, they can be separated again with a polarizer. As the fluence is on the order of 1 J/cm^2 a thin film polarizer has to be used, which provides the highest available damage threshold but has a poor extinction ratio (~200:1). A marginal misalignment—the two beams propagate under a small angle—allows blocking of the objectional energy, which has passed the polarizer, by the pinhole of the following spatial filter.

The ns-oscillator is a commercial Coherent Powerlite 8000. Due to its non-ideal elliptical transversal profile the beam is reshaped with a custom made cylinder telescope. After passing this optical system, the laser beam is circularly shaped. The improvement in terms of the spatial intensity distribution is shown in the images on the right-hand side of Figure 2.

Before transferring the ns-beam to the next amplification section, it is first spatially reshaped with a soft polarizing aperture (SPA). This SPA consists of a birefringent plano-convex lens, a second plano-concave BK-7 lens to compensate for the optical power of the first lens and a thin film polarizer. The linear polarization of the incoming beam is
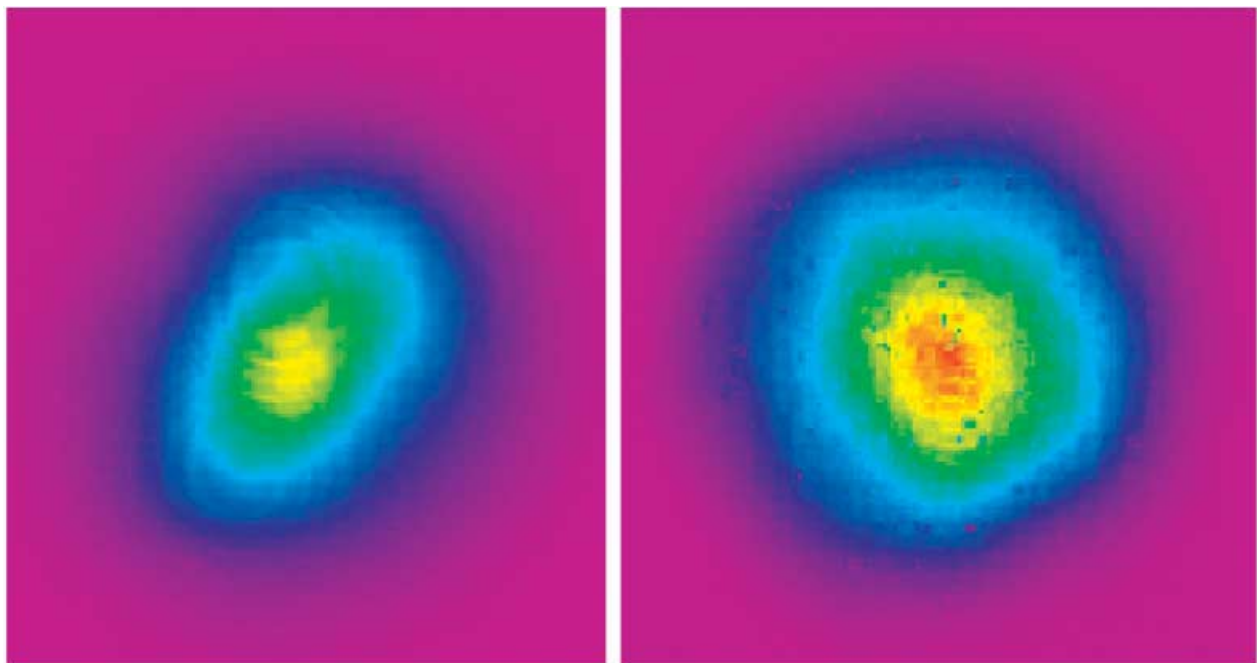

Fig. 2. Beamshape of the long pulse front-end: Oscillator profile before and after the cylinder telescope.

rotated according to the thickness of the birefringent lens. Taking into account the polarizer, the total power transmission of the SPA is now a function of the beam radius,

$$T(r) = \cos^2\left(\frac{1}{2}\,\Delta n\,\frac{\pi}{\lambda}\,\frac{r^2}{R}\right), \qquad (1)$$

where $\Delta n = 0.009$ denotes the difference between the refractive index of the ordinary and extraordinary wave; $\lambda = 1064$ nm is the laser wavelength, $R = 1197$ mm the radius of curvature of the birefringent lens, and $r \approx 12$ mm is the so called zero transmission radius, which depends on Δn, λ, and R. The calculated transmission is shown in Figure 3 together with the part of the beam that is reflected at the polarizer. One can clearly see the ring shaped intensity distribution, while the asymmetry is due to the inhomogeneous intensity distribution of the incoming beam.

Since the gain in rod amplifiers increases with radius due to absorption of the pump light on its way to the center of the rod, an initially Gaussian shaped intensity profile changes to a flat top like distribution along the amplifier chain. The SPA attenuates this effect, while it helps at the same time, to control diffraction at hard apertures in the laser chain.

The overall extracted energy strongly depends on the input beam profile and was measured to be on the order of 20%. As the maximum laser energy which can be extracted from the system is not limited by a lack of pump power, but by the damage threshold of the optical components, the loss of energy at the beam shaping element could easily be compensated by slightly increasing the pump power of the amplifiers.

After reshaping the beam with the SPA, it is relay-imaged to the double pass amplifier. Due to thermal induced birefringence of the amplifying media and the limited extinction ratio of the separating polarizer, there is always some part of the radiation propagating backward within the chain. To prevent damage, a faraday isolator with 25 mm clear aperture was integrated. The pulse is then guided to the booster section with a 45 mm and a 64 mm amplifier.

As long as the PHELIX laser beam is not yet available, the long pulse beam is used to produce a hot dense plasma, e.g., for energy loss experiments with electron temperatures in the order of 200 eV and electron densities up to solid state density. A small part of the sub-ns beam (some mJ) is coupled out and frequency doubled to probe the plasma by means of Wollaston interferometry. This diagnostic has recently been set up and provides a space resolved distribution of the free plasma electron density with time resolution given by the pulse length (0.5 ns) of the probe beam.

After the final amplification section for the sub-ns beam, which is realized as a geometrical triple pass, the pulse is expected to deliver 5 J of energy. This high power (10 GW) pulse can be focused on a medium-Z target that will serve as an X-ray backlighter. However there are plans to use higher harmonics of this beam for collective Thomson scattering (Glenzer, 2000). This will lead to new insights into the physics of the expanding plasma and it will serve as an alternative temperature diagnostics. Together with the PHELIX laser that will deliver up to 1 kJ laser energy in 1 ns, the new configuration of NHELIX will act as a powerful diagnostic laser system.

4. FAST PARTICLE GENERATION IN PLASMA JETS

The detailed analysis of laser generated plasmas was motivated by stopping power measurements of ionized matter. While energy loss measurement of ions in matter is an established research topic which has developed from a basic research into a field with numerous applications, the history of precise measurements of the stopping power of high energy heavy ions in plasma is relatively brief. Due to limited availability of powerful ion accelerators, this topic was addressed mainly in a few laboratories in France, Ger-
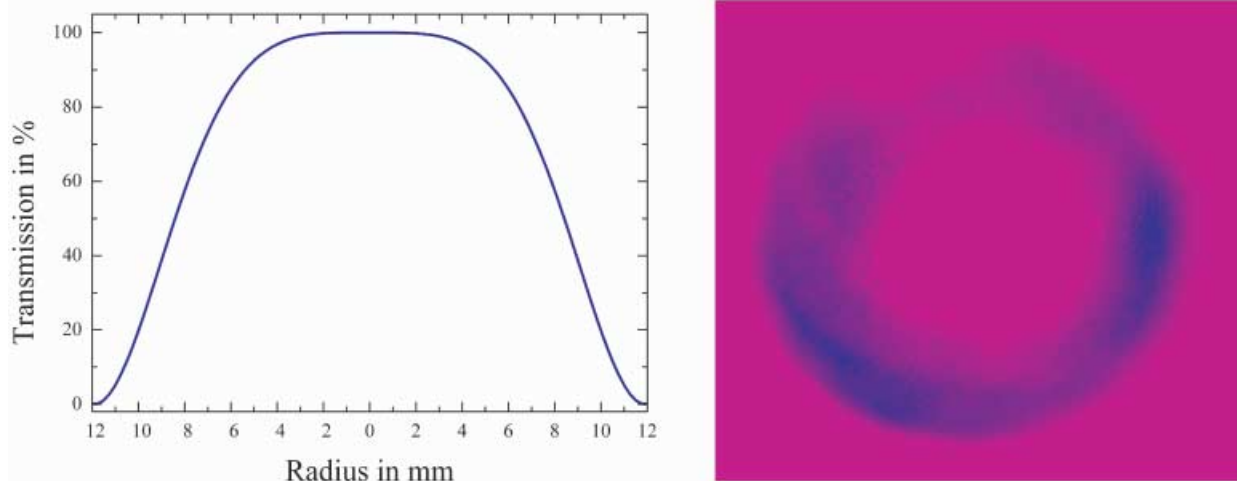

Fig. 3. Calculated transmission of the SPA and spatial distribution of the extracted energy.

many, Russia, and Japan. (Weyrich *et al*., 1989; Chabot *et al*., 1998; Golubev *et al*., 1998; Mintsev *et al*., 1999; Maynard *et al*., 2002; Kojima *et al*., 2002). The technique to measure the ion beam energy loss has reached a rather mature state; however, the precision of plasma parameter measurement is still limiting the overall experimental error margin. This is even more pronounced for transient laser plasma, where the transit time of the ion through the plasma is comparable to plasma dynamic time scale. Therefore it is of utmost necessity to measure the plasma parameters with time and spatial resolution, and to rely on plasma simulations where a detailed measurement is not yet possible.

The aim of the current experiment therefore was a detailed characterization of laser plasmas generated by the NHELIX facility for beam plasma interaction experiments. The results we report here were partly obtained before the NHELIX upgrade and in part after the completion of the upgrade described above, and we wanted to compare the reproducibility of observed effects.

For the previous experiment the NHELIX laser system was used with pulse duration of 15 ns and laser beam energy of between 12 J and 17 J only. The laser radiation was focused with a plane-convex lens (beam diameter 80 mm, focal length $f = 130$ mm) onto a solid Teflon target. The lens has a central aperture to let the ion beam pass through, for beam plasma interaction experiments. With a spot size of about 0.5 mm a comparatively low flux density of about 10^{12} W/cm^2 was achieved on the target. This constitutes an extremely extended plasma source. In order to obtain different laser fluxes on the target surface, the distance between the lens and the target was varied. In Figure 4a the experimental scheme is shown. The laser pulse is impinging onto the target from the right. A pinhole image with open shutter shows the development of a plasma plume which has a high directionality, and therefore, we refer to it as a plasma jet. This image was taken after the NHELIX upgrade. For comparison we show in Figure 4b an image taken before the upgrade, under almost similar conditions. Figure 4c shows a two pinhole image. Each pinhole has a diameter of 200 μm and shows the image of a laser generated C-plasma. One pinhole was covered with a polypropylene (1 μm)/Al (0.2μm) filter to take an image including the soft X-ray regime down to 300 eV and the other pinhole was covered with a 5 μm Ti filter for images in the hard X-ray regime above 1.5–2 keV. The hard X-rays consist of Bremsstrahlung mainly and show a predominantly cylindrical expansion of the plasma with an observed length of the plasma jet of about 30 mm, whereas the low energy image (above) is blurred by an expanding plasma cloud emitting low energy radiation.

The Bremsstrahlung emission is the dominating feature, indicating that the C-target is completely ionized. The demagnification factor of the image on the X-ray film is 3, the C-target has a thickness of 110 μm, and the images were taken with laser energy on the target of 100 J, a pulse length of 14 ns, and a laser focus of 2 mm. This corresponds to a laser intensity of 2.3×10^{11} W/cm^2. To our knowledge,

these results are the first observation of X-rays with more than 1.5 keV for such low laser flux intensity.

Both figures show a directional expansion of the plasma. Spectra were taken simultaneously under two different angles in order to be sensitive for Doppler shift effects. We attribute the jet phenomenon to ring shaped focus geometry, which was due to spherical aberrations of the final focusing lens with small f-number.

A similar effect was reported recently from the PALS laser facility in Prague (Jungwirth, 2005).

5. SPACE RESOLVED X-RAY SPECTROSCOPY

Within the non-invasive methods for plasma diagnostics, spectroscopy holds a prominent place.

X-ray spectroscopy of He-like and Li-like ions allows to probe the hot, dense region of the plasma, and to measure relevant plasma parameters like electron temperature and density. Moreover today's spectrometers allow high spectral resolution with space resolution at the same time. Thus it is possible to follow the energy loss and the charge state development of heavy ions moving inside a target with spectromicroscopic methods (Rosmej *et al*., 2002). The necessity of spatial resolution led to the development of focusing spherically bent crystal spectrometers with spectral resolution (FSSR) (Faenov *et al*., 1994). This crystal geometry simultaneously allows to cover a large spectral range and obtaining spectra simultaneously with high spectral ($\lambda/\Delta\lambda = 4.000$) and with high spatial resolution ($\Delta x = 20$–40 μm). The FSSR spectrometer can work in two configurations: With one-dimensional (1D) spatial resolution perpendicular to the direction of the spectral one and with two-dimensional (2D) spatial resolution—the second spatial resolution is in the direction of dispersion. The maximum spectral resolution is obtained in the 1D scheme. This requires the crystal and the detector to be placed on the Rowland circle, analogue to the Johann scheme for cylindrically bent crystal spectrometers. For the spatial resolution the respective distances of the crystal to the emitting source and the crystal to the detector follow the simple equations,

$$a = R \cos \varphi / \cos 2\varphi \qquad (2)$$

$$b = R \cos \varphi,$$

where φ is the Bragg-angle subtended by the crystal plane and the emission source, a is the distance crystal-source and b the distance from the crystal to the detector. In the 2D scheme the detector is placed outside the Rowland circle. Therefore two spatial dimensions can be observed simultaneously. The determination of the respective geometrical parameters is more complicated in this case, than in the 1D case (Young *et al*., 1998). One should note that the spectral resolution in the 1D-case does not depend on the plasma size. In Figure 5, a scheme of both possibilities is presented.
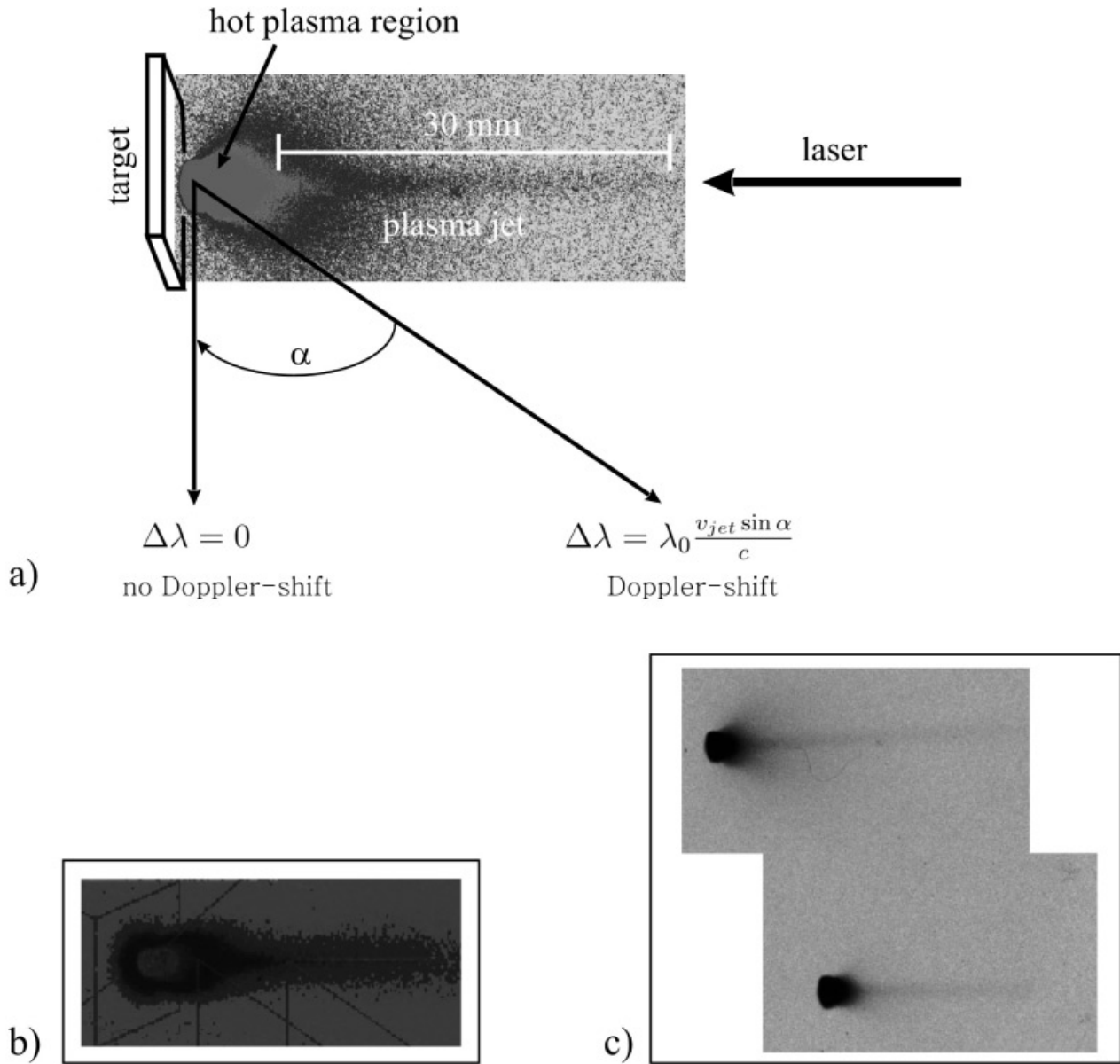
Fig. 4. Scheme of the spectroscopic ion energy measurement using the Doppler shift method (Rosmej *et al.*, 1999). (**a**) The image shows the actual set-up. The laser energy was up to 100 J and the plasma was investigated with a pinhole camera and two spatially resolving spectrometers with a high spectral resolution. One spectrometer was placed in a way, that it observed the plasma from 0° to the target surface, while the other spectrometer was positioned with a large angle to detect a possible Doppler-shift of the fast ions. The image in the background shows a plasma jet of approx. 30 mm length. (**b**) This pinhole image was taken before the NHELIX upgrade. (**c**) Carbon plasma image of a dual pinhole camera. The lower 200 μm pinhole was covered with 5 μm Ti, the upper 200 μm with 1 μm C_3H_6 + 0.2 μm Al. The expanded plasma has a compact cylindrical expansion in laser direction.

6. EXPERIMENTAL RESULTS

The spherically bent crystals, which allow spatial and spectral resolution in the X-ray regime, open the possibility to observe the plasma ion behavior beyond the critical density, and thus provide a probe for the hot spot region.

The presence of high energy ions well above the thermal energy in plasmas which are created by long pulsed lasers over thick targets was confirmed in different facilities, including the NHELIX laser at GSI (Rosmej *et al.*, 2002*a*; 2002*b*). The effect was proven with the Doppler X-ray spectroscopic method (Rosmej *et al.*, 1999). By means of two FSSR with different angles to the target direction the Doppler shift is quantifiable. One of the spectrometers is placed perpendicular to the laser beam axis, which is also perpendicular to the main plasma expansion direction. A second FSSR is placed under a large angle with respect to the target surface.
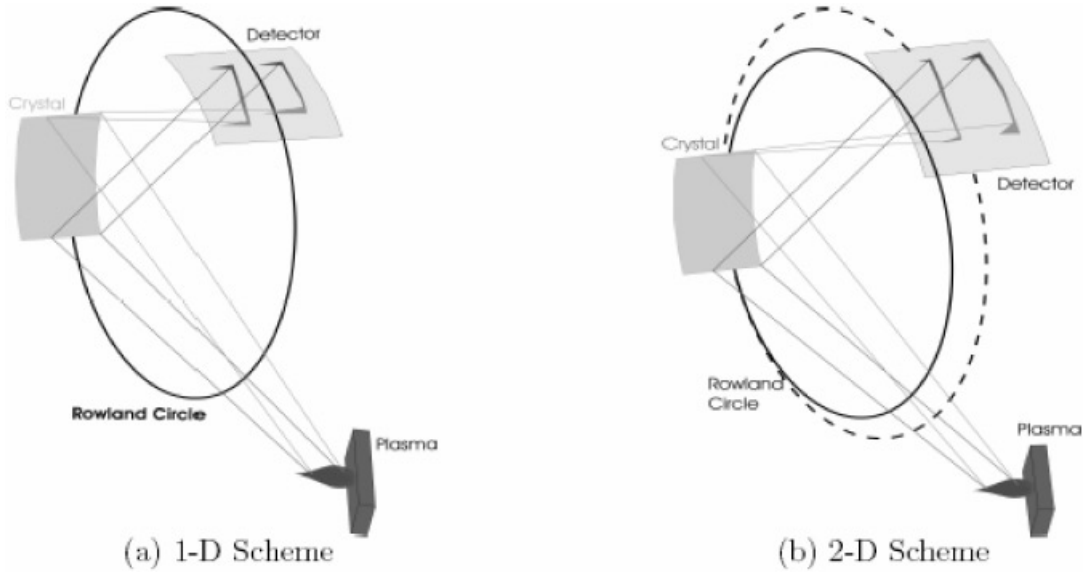
Fig. 5. FSSR scheme. (**a**) one-dimensional setup, where the detector is placed on the Rowland circle. (**b**) two dimensional setup, where the detector is placed outside the Rowland circle.

The comparison of both spectra allows the detection of Doppler-shifted spectral lines. If the ions are moving with a high velocity out of the plasma, their emitted spectral lines will have a blue Doppler-shift. This shift $\Delta\lambda$ can be related to the ion's velocity according to:

$$\Delta\lambda = \lambda_0 \frac{v_{jet}\sin\alpha}{c}. \tag{3}$$

Here $\tilde{\lambda}$ is the un-shifted line in the ion's reference system, v_{jet} the velocity of the ions, α the angle with respect to the target surface and c the light velocity.

Since the observed velocities are small with respect to the velocity of light the relativistic Doppler effects does not play any role for the spectra measured in perpendicular direction to the jet expansion. Figure 6 shows the results of the recent experiments compared to the data from experiments before the NHELIX upgrade taken from (Rosmej *et al.*, 1999). In the fluorine spectra from (Rosmej *et al.*, 1999) the line shape of the Ly_α line measured in 55° is clearly different from the line measured in 5°. This strong blue asymmetry was explained as a result of the expansion dynamics that correspond in large Doppler shifts from non-thermal expansion. The symmetric line profile from the line recorded in 5° shows that the motion of fast ions occurred normal to the surface. The arrow in the image corresponds to the Doppler-shift that ions with 3.6 MeV will produce.

We wanted to point out that the measured energy in this case is well above the energy expected by the Gitomer scaling curve. Whereas at $I\lambda^2 = 10^{12}$ Wcm^{-2} μm^2 we measure a maximum energy well above 3 MeV, the scaling by Gitomer would predict 30–50 keV only.

Our recent experiments were performed with the aim to explore the relation of the suprathermal ion energy and the laser intensity, using the NHELIX laser at GSI. The targets were massive Mg-disks. In the new set-up after the NHELIX upgrade we used two FSSRs with detection angles of 4° and 25°, respectively. Their wavelength range were set to cover the resonance line He_α (w), inter-combination line y and dielectronic satellites $1s2lnl' \rightarrow 1s^2nl''$ (Gabriel, 1972). The spectra are shown in Figure 6b. The laser energy was 45–50 J, corresponding to 5×10^{12} W/cm^2 at the position of the smallest possible focus. With a moderate spectral resolution of $\tilde{\lambda}\Delta\lambda = 2000$ and Eq. (3) ions with kinetic energies of more than 160 keV can be detected with the Doppler spectroscopy. However, no Doppler shift asymmetry of the emission lines was detected in this case. Anyhow we could not observe a plasma jet in the x-ray pinhole image, too.

7. CONCLUSION

The existence of ion energies well above the Gitomer scaling was observed in many experiments. At higher laser intensities this may well be attributed to relativistic self focusing (Hora, 1975; Ehler, 1975), and the effect of relativistic self-focusing or of its suppression is of utmost importance for plasma block generation, which is currently discussed also for a new fusion scheme in current literature (Osman *et al.*, 2004; Hora, 2004, 2005; Wilks, 2005; Badziak *et al.*, 2005). The exact cause of the observed plasma jets is not known for this experiment. Detailed parameter studies of future planned experiments will probably give more insight.

In the experiment we present here, we did not detect the particles with a particle detector far away from the target. On the contrary we used spectroscopic methods to detect the high energy ions at their place of origin. It is well known that plasmas are a very efficient medium to slow down energetic
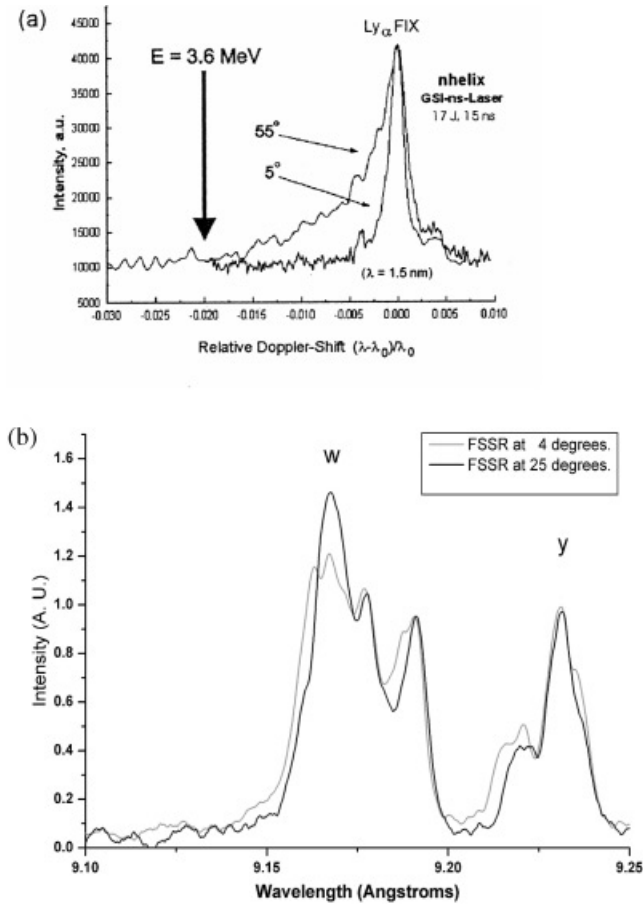
Fig. 6. Experimental data measured with two FSSR. (**a**) The spectrum taken at 55° shows a strong asymmetric line profile due to the Doppler shift of high energetic ions (Rosmej *et al.*, 1999). (**b**) Spectra from recent experiments with Mg. The asymmetry one the red side of the He_α resonance line w (Gabriel, 1972) is due to higher orders dielectronic satellites: $1s2lnl' \rightarrow 1s^2nl''$. There is no asymmetry on the blue side visible hence there is no Doppler shift.

heavy ions. Therefore it comes as no surprise to us that the energy we measure with spectroscopic methods is higher than the energy measured with particle detectors. However, the underlying mechanism for these energies to occur is still unclear. We therefore propose to do systematic studies for the possibility of acceleration of MeV ions using ns-laser pulses with reasonably low laser intensities at different laser laboratories to investigate this effect and apply particle detection and spectroscopic methods at the same time. Most suitable for this kind of measurement campaign seem to be the laser installation PALS in Prague and NHELIX/PHELIX at GSI-Darmstadt.

ACKNOWLEDGMENT

REFERENCES

ALEXEEV, N.N., ALEKSEEV, P.N., BALANUTSA, V.N., BEREZNITSKY, S.L., EVTICHOVICH, V.N., GORJACHEV, J.M., KIRILLOV, A., KOSHKAREV, D.G., MESCHEREKOV, N.D., MILUACHENKO, A.V., NIKITIN, G.A., NIKOLAEV, V.I., OKOROKOV, I.S., SHARKOV, B.Y., SCHEGOLEV, V.A., SOSNIN, D.V., SHUMSHUROV, A., VESELOV, M.A., ZAVODOV, V.P., ZAVRAZHNOV, V.S., ZENKEVICH, P.R., ZHURAVLEV, A.S., MAMAEV, G.L., KRASNOPOLSKY, V.A., KRYLOV, S.J., PUCHKOV, S.N. & TENJAKOV, I.E. (2002). Status of the Terawatt Accumulator Accelerator project. *Laser Part. Beams* **20**, 385–391.

BADZIAK, J., GLOWACZ, S., JABLONSKI, S., PARYS, P., WOLOWSKI, J. & HORA, H. (2005). Laser driven generation of high-current ion beams using skin-layer ponderomotive acceleration. *Laser Part. Beams* **23**, 401–409.

BALAKIREV, V.A., KARAS, I.V., KARAS, V.I., LEVCHENKO, V.D. & BONATICI, M. (2004). Charged particle acceleration by an intense wake-field excited in plasmas by either laser pulse or relativistic electron bunch. *Laser Part. Beams* **22**, 383–392.

CHABOT, M., NECTOUX, M., GARDES, D., MAYNARD, G. & DEUTSCH, C. (1998). Charge state dependence of the stopping power for chlorine ions interacting with a cold gas and a plasma (1.5 MeV/u). *Nucl. Instr. Meth. Phys. Res.* **415**, 571–575.

DIETRICH, K.G., HOFFMANN, D.H.H., BOGGASCH, E., JACOBY, J., WAHL, H., ELFERS, M., HAAS, C.R., DUBENKOV, V.P. & GOLUBEV, A.A. (1992). Charge state of fast heavy-ions in a hydrogen plasma. *Phys. Rev. Lett.* **69**, 3623–3626.

EHLER, A.W. (1975). High-energy ions form CO_2 laser-produced plasma. *J. Appl. Phys.* **45**, 2464–2467.

FAENOV, A.Y., PIKUZ, S.A., ERKO, A.I., BRYUNETKIN, B.A., DYAKIN, V.M., IVANENKOV, G.V., MINGALEEV, A.R., PIKUZ, T.A., ROMANOVA, V.M. & SHELKOVENKO, T.A. (1994). High-performance x-ray spectroscopic devices for plasma microsources investigations. *Phys. Scripta* **50**, 333–338.

FUKUDA, Y., AKAHANE, Y., AOYAMA, M., INOUE, N., UEDA, H., KISHIMOTO, Y., YAMAKAWA, K., FAENOV, A.Y., MAGUNOV, A.I., PIKUZ, T.A., SKOBELEV, I.Y., ABDALLAH, J., CSANAK, G., BOLDAREV, A.S. & GASILOV, V.A. (2004). Generation of X rays and energetic ions from superintense laser irradiation of micronsized Ar clusters. *Laser Part. Beams* **22**, 215–220.

GABRIEL, A.H. (1972). Dielectronic satellite spectra for highly-charged helium-like ion lines. *Royal Astronomical Soc.* **160**, 99.

GITOMER, S.J., JONES, R.D., BEGAY, F., EHLER, A.W., KEPHART, J.F. & KRISTAL, R. (1986). Fast ions and hot-electrons in the laser-plasma interaction. *Phys. Fluids* **29**, 2679–2688.

GLENZER, S.H. (2000). Thomson scattering in inertial confinement fusion research. *Contrib. Plasma Phys.* **40**, 36–45.

GLENZER, S.H., GREGORI, G., LEE, R.W., ROGERS, F.J., POLLAINE, S.W. & LANDEN, O.L. (2003). Demonstration of spectrally resolved X-ray scattering in dense plasmas. *Phys. Rev. Lett.* **90** (17).

GLENZER, S.H., GREGORI, G., ROGERS, F.J., FROULA, D.H., POLLAINE, S.W., WALLACE, R.S. & LANDEN, O.L. (2003). X-ray scattering from solid density plasmas. *Phys. Plasmas* **10**, 2433–2441.

GOLUBEV, A., BASKO, M., FERTMAN, A., KOZODAEV, A., MESHERYAKOV, N., SHARKOV, B., VISHNEVSKIY, A., FORTOV, V., KULISH, M., GRYAZNOV, V., MINTSEV, V., GOLUBEV, E., PUKHOV, A., SMIRNOV, V., FUNK, U., STOEWE, S., STETTER, M., FLIERL, H.P., HOFFMANN, D.H.H., JACOBY, J. & IOSILEVSKI,

I. (1998). Dense plasma diagnostics by fast proton beams. *Phys. Rev. E* **57**, 3363–3367.

GREGORI, G., GLENZER, S.H., ROGERS, F.J., POLLAINE, S.M., LANDEN, O.L., BLANCARD, C., FAUSSURIER, G., RENAUDIN, P., KUHLBRODT, S. & REDMER, R. (2004). Electronic structure measurements of dense plasmas. *Phys. Plasmas* **11**, 2754–2762.

HASEGAWA, J, YOKOYA, N., KOBAYASHI, Y., YOSHIDA, M., KOJIMA, M., SASAKI, T., FUKUDA, H., OGAWA, M., OGURI, Y. & MURAKAMI, T. (2003). Stopping power of dense helium plasma for fast heavy ions. *Laser Part. Beams* **21**, 7–11.

HASEROTH, H. & HORA, H. (1996). Physical mechanisms leading to high currents of highly charged ions in laser-driven ion sources. *Laser Part. Beams* **14**, 393–438.

HOFFMANN, D.H.H., BLAZEVIC, A., NI, P., ROSMEJ, O., ROTH, M., TAHIR, N.A., TAUSCHWITZ, A., UDREA, S., VARENTSOV, D., WEYRICH, K. & MARON, Y. (2005). Present and future perspectives for high energy density physics with intense heavy ion and laser beams. *Laser Part. Beams* **23**, 47–53.

HOFFMANN, D.H.H., BOCK, R., FAENOV, A.Y., FUNK, U., GEISSEL, M., NEUNER, U., PIKUZ, T.A., ROSMEJ, F., ROTH, M., SUSS, W., TAHIR, N. & TAUSCHWITZ, A. (2000). Plasma physics with intense laser and ion beams. *Nuc. Instr. Meth. Phys. Res.* **161**, 9–18.

HOFFMANN, D.H.H., WEYRICH, K., WAHL, H., GARDES, D., BIMBOT, R. & FLEURIER, C. (1990). Energy-loss of heavy-ions in a plasma target. *Phys. Rev. A* **42**, 2313–2321.

HORA, H. (1975). Theory of relativistic self-focusing of laser radiation in plasmas. *J. Opt. Soc. Am.* **65**, 882–886.

HORA, H. (2004). Developments in inertial fusion energy and beam fusion at magnetic confinement. *Laser Part. Beams* **22**, 439–449.

HORA, H. (2005). Difference between relativistic petawatt-picosecond laser-plasma interaction and subrelativistic plasma-block generation. *Laser Part. Beams* **23**, 441–451.

JACOBY, J., HOFFMANN, D.H.H., LAUX, W., MULLER, R.W., WAHL, H., WEYRICH, K., BOGGASCH, E., HEIMRICH, B., STOCKL, C., WETZLER, H. & MIYAMOTO, S. (1995). Stopping of heavy-ions in a hydrogen plasma. *Phys. Rev. Lett.* **74**, 1550–1553.

JUNGWIRTH, K. (2005). Recent highlights of the PALS research programme. *Laser Part. Beams* **23**, 177–182.

KHAYDAROV, R.T., BERDIYOROV, G.R., KUNISHEV, U., KHALMURATOV, M., TOJIKHONOV, M.E. & KANAPATHIPILLAI, M. (2005). Investigation of PbMg target characteristics by a laser mass-spectrometer. *Laser Part. Beams* **23**, 521–526.

KOJIMA, M., MITOMO, M., SASAKI, T., HASEGAWA, J. & OGAWA, M. (2002). Charge-state distribution and energy loss of 3.2-MeV oxygen ions in laser plasma produced from solid hydrogen. *Laser Part. Beams* **20**, 475–478.

KOSHKAREV, D.G. (2002). Heavy ion driver for fast ignition. *Laser Part. Beams* **20**, 595–598.

MAGUNOV, A.I., FAENOV, A.Y., SKOBELEV, I.Y., PIKUZ, T.A., DOBOSZ, S., SCHMIDT, M., PERDRIX, M., MEYNADIER, P., GOBERT, O., NORMAND, D., STENZ, C., BAGNOUD, V., BLASCO, F., ROCHE, J.R., SALIN, F. & SHARKOV, B.Y. (2003). X-ray spectra of fast ions generated from clusters by ultrashort laser pulses. *Laser Part. Beams* **21**, 73–79.

MALKA, V. & FRITZLER, S. (2004). Electron and proton beams produced by ultra short laser pulses in the relativistic regime. *Laser Part. Beams* **22**, 399–406.

MAYNARD, G., DEUTSCH, C., GARDES, D. & CHABOT, M. (2002).

Energy loss of MeV/n heavy ions in dense hydrogen plasmas. *Plasma Sour. Sci. Techn.* **11**, A131–A137.

MINTSEV, V., GRYAZNOV, V., KULISH, M., FILIMONOV, A., FORTOV, V., SHARKOV, B., GOLUBEV, A., FERTMAN, A., TURTIKOV, V., VISHNEVSKIY, A., KOZODAEV, A., HOFFMANN, D.H.H., FUNK, U., STOEWE, S., GEISEL, M., JACOBY, J., GARDES, D. & CHABOT, M. (1999). Stopping power of proton beam in a weakly nonideal xenon plasma. *Contr. Plasma Phys.* **39**, 45–48.

NEUMAYER, P., SEELIG, W., CASSOU, K., KLISNICK, A., ROS, D., URSESCU, D., KUEHL, T., BORNEIS, S., GAUL, E., GEITHNER, W., HAEFNER, C. & WIEWIOR, P. (2004). Transient collisionally excited X-ray laser in nickel-like zirconium pumped with the PHELIX laser facility. *Appl. Phys. B-Lasers Opt.* **78**, 957–959.

NEUMAYER, P., BOCK, R., BORNEIS, S., BRAMBRINK, E., BRAND, H., CAIRD, J., CAMPBELL, E.M., GAUL, E., GOETTE, S., HAEFNER, C., HAHN, T., HEUCK, H.M., HOFFMANN, D.H.H., JAVORKOVA, D., KLUGE, H.-J., KUEHL, TH., KUNZER, S., MERZ, T., ONKELS, E., PERRY, M.D., REEMTS, D., ROTH, M., SAMEK, S., SCHAUMANN, G., SCHRADER, F., SEELIG, W., TAUSCHWITZ, A., THIEL, R., URSESCU, D., WIEWIOR, P., WITTROCK, U. & ZIELBAUER, B. (2005). Status of PHELIX Laser and First Experiments. *Laser Part. Beams* **23**, 385–389.

OGAWA, M., YOSHIDA, M., NAKAMIJA, M., HASEGAWA, J., FUKATA, S., HORIOKA, K. & OGURI, Y. (2003). High-current laser ion source based on low-power laser. *Laser Part. Beams* **21**, 633–640.

OSMAN, F., HORA, H., CANG, Y., EVANS, P., CAO, H., LIU, H., HE, X.T., BADZIAK, J., PARYS, A.B., WOLOWSKI, J., WORYNA, E., JUNGWIRTH, K., KRALIKOVA, B., KRASKA, J., LASKA, L., PFEIFER, M., ROHLENA, K., SKALA, J. & ULLSCHMIED, J. (2004). Skin depth plasma front interaction mechanism with prepulse suppression to avoid relativistic self focusing for high gain laser fusion. *Laser Part. Beams* **22**, 83–88.

PEGORARO, F., ATZENI, S., BORGHESI, M., BULANOV, S., ESIREKEPOV, T., HONRUBIA, J., KATO, Y., KHOROSHKOV, V., NISHIHARA, K., TAJIMA, T., TEMPORAL, M. & WILLI, O. (2004). Production of ion beams in high-power laser-plasma interactions and their application. *Laser Part. Beams* **22**, 19–24.

PENACHE, D., NIEMANN, C., TAUSCHWITZ, A., KNOBLOCH, R., NEFF, S., BIRKNER, R., GEISSEL, M., HOFFMANN, D.H.H., PRESURA, R., PENACHE, C., ROTH, M. & WAHL, H. (2002). Experimental investigation of ion beam transport in laser initiated plasma channels. *Laser Part. Beams* **20**, 559–563.

RAFIQUE, M.S., RAHMAN, M.K., ANWAR, M.S., ASHFAD, F.M.A. & SIRAJ, K. (2006). Angular distribution and forward peaking of laser produced plasma ions. *Laser Part. Beams* **24**. In press.

ROSMEJ, F.B., HOFFMANN, D.H.H., SUESS, W., GEISSEL, M., PIRZADEH, P., ROTH, M., SEELIG, W., FAENOV, A.Ya, SKOBELEV, I.Yu, MAGUNOV, A.I, PIKUZ, T.A, BOCK, R., FUNK, U.N., NEUNER, U., UDREA, S., TAUSCHWITZ, A., TAHIR, N.A., SHARKOV, B.Yu. & ANDREEV, N.E. (1999). Observation of MeV ions in long-pulse, large-scale laser-produced plasmas. *JETP Lett.* **70**, 270–276.

ROSMEJ, F.B., RENNER, O., KROUSKY, E., WIESER, J., SCHOLLMEIER, M., KRASA, J., LASKA, L., KRALIKOVA, B., SKALA, J., BODNAR, M., ROSMEJ, O.N. & HOFFMANN, D.H.H. (2002a). Space-resolved analysis of highly charged radiating target ions generated by kilojoule laser beams. *Laser Part. Beams* **20**, 555–557.

ROSMEJ, F.B., HOFFMANN, D.H.H., SUSS, W., STEPANOV, A.E., SATOV, Y.A., SMAKOVSKII, Y.B., ROERICH, V.K., KHOMENKO, S.V., MAKAROV, K.N., STAROSTIN, A.N., FAENOV, A.Y., SKOBELEV, I.Y., MAGUNOV, A.I., GEISSEL, M., PIRZADEH, P., SEELIG, W.,

PIKUZ, T.A., BOCK, R., LETARDI, T., FLORA, F., BOLLANTI, S., DI LAZZARO, P., REALE, A., SCAFATI, A., TOMASSETTI, G., AUGUSTE, T., D'OLIVEIRA, P., HULIN, S., MONOT, P. & SHARKOV, B.Y. (2002*b*). The generation of fast particles in plasmas created by laser pulses with different wavelengths. *J. Exp. Theo. Phys.* **94**, 60–72.

ROSMEJ, O.N., WIESER, J., GEISSEL, M., ROSMEJ, F., BLAKEVIC, A., JACOBY, J., DEWALD, E., ROTH, M., BRAMBRINZ, E., WEYRICH, K., HOFFMANN, D.H.H., PIKUZ, T.A., FAENOV, A.Y., MAGUNOV, A.I., SKOBELEV, I.Y., BORISENKO, N.G., SHEVELKO, V.P., GOLUBEV, A.A., FERTMAN, A., TURTIKOV, V. & SHARKOV, B.Y. (2002). X-ray spectromicroscopy of fast heavy ions and target radiation. *Nucl. Instr. Meth. Phys.* **495**, 29–39.

ROTH, M., STOCKL, C., SUSS, W., IWASE, O., GERICKE, D.O., BOCK, R., HOFFMANN, D.H.H., GEISSEL, M. & SEELIG, W. (2000). Energy loss of heavy ions in laser-produced plasmas. *Europhys. Lett.* **50**, 28–34.

SHARKOV, B.YU. (2002). Guest editors Preface: 14th international heavy ion inertial fusion symposium, and references therein. *Laser Part. Beams* **20**, 367.

SHOROKHOV, O. & PUKHOV, A. (2004). Ion acceleration in over-dense plasma by short pulse laser. *Laser Part. Beams* **22**, 175–182.

STEPANOV, A.E., VOLKOV, G.S., ZAITSEV, V.I., MAKAROV, K.N., SATOV, YU.A. & ROERICH, V.C. (2002). Measurement of temperature evolution for the laser ion source plasma. *Laser Part. Beams* **20**, 613.

VARENTSOV, D., TAHIR, N.A., LOMONOSOV, I.V., HOFFMANN, D.H.H., WIESER, J. & FORTOV, V.E. (2003). Energy loss dynamics of an intense uranium beam interacting with solid neon for equation-of-state studies. *Europhys. Lett.* **64**, 57–63.

WILKS, S.C. (2005). Energetic proton generation in ultra-intense laser solid interaction and target normal aheath acceleration. *Laser Part. Beams* **23(4)**.

YOUNG, B.K.F., WILSON, B.G., PRICE, D.F. & STEWART, R.E. (1998). Measurement of X-ray emission and thermal transport in near-solid-density plasmas heated by 130 fs laser pulses. *Phys. Rev. E* **58**, 4929–4936.

ZHIDKOV, A.G., SASAKI, A., TAJIMA, T., AUGUSTE, T., D'OLIVEIRA, P., HULIN, S., MONOT, P., FAENOV, A.YA., PIKUZ, T.A. & SKOBELEV, I.YU. (1999). Direct spectroscopic observation of multiple charged ion acceleration by intense femtosecond pulse laser. *Phys. Rev. E.* **60**, 3273.